

## Mathematical Modelling of MHD Unsteady heat and mass transfer of a Micropolar fluid past a vertical semi-infinite porous inclined plate and magnetic field with Soret and Dufour effects

Mutua Nicholas Muthama\*, Kinyanjui Mathew Ngugi\*\*, Kwanza Jackson Kioko\*\*\*, Gatheri Francis Kimani\*\*\*\*

\**(Department of Mathematics, Statistics & Physical Sciences, Taita Taveta University, Kenya, Voi-635-80300*

\*\* *(Department of Pure & Applied Mathematics, Jomo Kenyatta University of Agriculture & Technology, Kenya, Nairobi-62000-00200*

\*\*\* *(Department of Pure & Applied Mathematics, Jomo Kenyatta University of Agriculture & Technology, Kenya, Nairobi-62000-00200*

\*\*\*\* *School of Mathematics and Statistics, Technical University of Kenya, Kenya, Nairobi-52428-00200*

*Corresponding Author: Mutua Nicholas Muthama*

### ABSTRACT

The present study investigates the effects of Soret and Dufour on unsteady MHD heat and mass transfer flow of a Micropolar fluid past a vertical semi-infinite porous inclined plate in presence of an inclined Magnetic field. The resulting non-linear coupled Partial Differential Equations are solved by the Trivariate Spectral Collocation Method (TSCM). The results of velocity, angular momentum, temperature and concentration profiles are presented graphically and discussed after varying the various parameters. The various engineering quantities of interest including skin friction, couple stress, rate of heat and mass transfer are numerically evaluated and discussed.

**Keywords** – Couple stress, heat transfer, inclined magnetic field, mass transfer, Skin friction, Unsteady.

Date of Submission: 28-02-2019

Date of acceptance: 25-03-2019

### I. INTRODUCTION

The micropolar hydrodynamics is applied to describe the behaviour of magnetic liquids, polymer suspensions, liquid crystals, and other types of fluids with microstructure. Within the Cosserat continuum theory, many problems were successfully solved. One of the principal difficulties of any micropolar theory is to establish its constitutive equations. This question was not discussed in the Cosserats' original monograph, and it was a reason why the ideas of micropolar continuum were not recognized by many researchers. But even if for a material the constitutional equations are formulated, we are faced with a new hard problem: the identification of the material parameters.

[1] investigated micropolar fluid over a stretching surface in a non-Darcian porous medium when viscosity and thermal conductivity vary with temperature in presence of magnetic field. [2] was the first to formulate the theory of micro polar fluids. In essence, the theory introduces new material parameters, an additional independent vector field, the micro rotation and new constitutive equations, which must be solved simultaneously with the usual equations for Newtonian flow. The desire to model the non-Newtonian flow of fluid containing rotating

micro-constituents provided initial motivation for the development of the theory, but subsequent studies have successfully applied the model to a wide range of applications including blood flow, lubricants, porous media, turbulent shear flows and flowing capillaries and micro channels [3].

[4] analyzed Melting Heat Transfer and Induced-Magnetic Field Effects on the Micropolar Fluid Flow towards Stagnation Point using Boundary Layer Analysis. Their results indicated that due to the formation of boundary layer on melting surface (region of low heat energy) in the presence of induced magnetic field, space and temperature dependent internal heat generation enhances the heat transfer rate. [13] explored the Chemical reaction and thermal radiation effects on MHD micropolar fluid past a stretching sheet embedded in a non-Darcian porous medium. It was established that the increase in Schmidt number and chemical reaction caused a decrease in the skin-friction coefficient and an increase in the mass transfer rate.

[5] studied Similarity Solution of Unsteady Boundary Layer Flow of Nanofluids past a Vertical Plate with Convective Heating. It was inferred that the velocity and temperature of nanofluid decreases

as a result of increasing unsteadiness parameter while the velocity and the temperature distributions decrease by decreasing Biot number. Effects of Variable Viscosity and Thermal Conductivity of Unsteady Micropolar Fluid under Mixed Convection in Presence of Uniform Magnetic Field on Stretching Surface was studied by [6]. In their study it was observed that within the boundary layer thermal conductivity and viscosity parameter along with other parameters have a significant effect on velocity, micro-rotation, temperature distribution and magnetic field.

[7] researched on MHD and radiation effects on mixed convection unsteady flow of micropolar fluid over a stretching sheet. They found out that there is a smooth transition from small-time solution to the large-time solution. The Numerical study of MHD micropolar Carreau nanofluid in the presence of induced magnetic field was carried out by [8]. It was noted that the dimensionless velocity is enhanced for the Weissenberg number and the power law index while reverse situation is studied in the thermal and the concentration profile.

[9] investigated Soret and Dufour Effects on Steady free Convection in MHD Micropolar Fluid Flow, Mass and Heat Transfer with Hall Current. It was observed that the temperature profile increases as Pr and Df increases

### 1.1 ASSUMPTIONS AND APPROXIMATIONS

1. The flow is unsteady and laminar
2. The velocity vector is of the form  $\vec{q} = (u, 0, w)$
3. A strong transverse magnetic field which makes an angle  $\psi$  with the inclined plate and the vertical is applied
4. All the physical properties of the fluid are considered to be constant
5. All velocities are small compared with that of light  $\frac{q^2}{c^2} \ll 1$
6. Thermal conductivity  $\kappa$  is assumed constant

### 1.2 MATHEMATICAL FORMULATION

In the current study, we consider a two-dimensional, unsteady, viscous, electrically conducting, heat and mass transfer of micropolar fluid flow through porous medium past a vertical semi-infinite inclined porous plate in the presence of variable magnetic field, suction/injection, Soret and Dufour effects. The semi-infinite vertical porous plate is inclined along the z-axis, y-axis is perpendicular to the inclined plate as depicted in figure 1. A variable magnetic field  $B$  inclined at angle  $\psi$  is applied transversely along the y-axis and perpendicular to z-axis. The plate and the micropolar fluid are maintained at same temperature and

concentration initially, instantaneously raised to a temperature  $T_w (> T_\infty)$  and concentration  $C_w (> C_\infty)$  which remains constant.

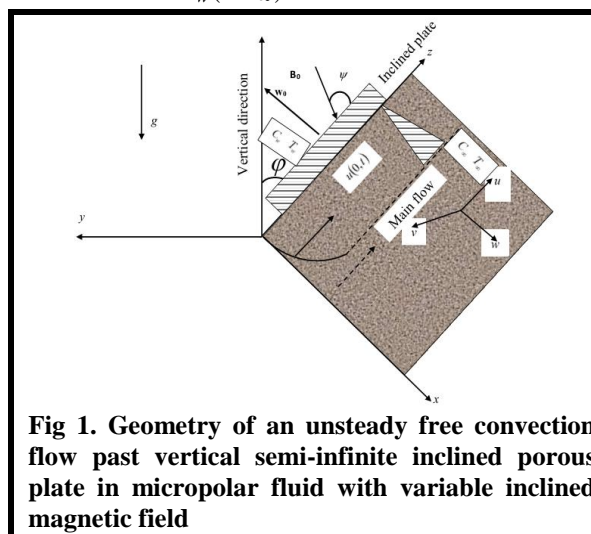


**Fig 1. Geometry of an unsteady free convection flow past vertical semi-infinite inclined porous plate in micropolar fluid with variable inclined magnetic field**

The magnetic field is resolved as follows;

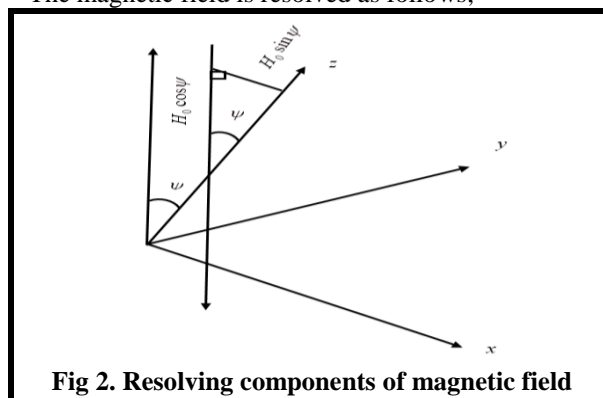


**Fig 2. Resolving components of magnetic field**

From figure 2 above, we have;

$$\sin \psi = \frac{y\text{-component}}{H_0} \Rightarrow y\text{-component} = H_0 \sin \psi$$

and

$$\cos \psi = \frac{x\text{-component}}{H_0} \Rightarrow x\text{-component} = H_0 \cos \psi$$

By the above physical conditions, the governing boundary layer and Boussinesq's approximations, the fundamentals equations are;

Mass Conservation Equation

$$\frac{\partial u}{\partial x} + \frac{\partial w}{\partial z} = 0 \quad (1)$$

Linear Conservation Equation

$$\frac{\partial u}{\partial t} + u \frac{\partial u}{\partial x} + w \frac{\partial u}{\partial z} = \left( \frac{\mu + k}{\rho} \right) \frac{\partial^2 u}{\partial z^2} + \left( \frac{k}{\rho} \right) \frac{\partial N}{\partial z} + g_a [\beta(T - T_\infty) + \beta'(C - C_\infty)] \cos \psi - \frac{\sigma B_0^2 \sin^2 \psi}{\rho} u - \frac{\nu u}{\rho K_p} \quad (2)$$

Equation of Angular Momentum

$$\rho j \left( \frac{\partial N}{\partial t} + u \frac{\partial N}{\partial x} + w \frac{\partial N}{\partial z} \right) = \gamma \frac{\partial^2 N}{\partial z^2} - k \left( 2N + \frac{\partial u}{\partial t} \right) \quad (3)$$

Equation of Energy

$$\frac{\partial T}{\partial t} + u \frac{\partial T}{\partial x} + w \frac{\partial T}{\partial z} = \frac{k'}{\rho j} \frac{\partial^2 T}{\partial z^2} + \frac{\nu}{C_p} \left( \frac{\partial u}{\partial z} \right)^2 + \frac{D_m k_T}{C_s C_p} \frac{\partial^2 C}{\partial z^2} \quad (4)$$

Species Concentration Equation

$$\frac{\partial C}{\partial t} + u \frac{\partial C}{\partial x} + w \frac{\partial C}{\partial z} = D_m \frac{\partial^2 C}{\partial z^2} + \frac{D_m k_T}{T_m} \frac{\partial^2 T}{\partial z^2} \quad (5)$$

Defining the associated the associated Boundary Conditions on the semi-infinite vertical plate as:

$$\left. \begin{aligned} u(x,0,t) = U_w(x,0,t) = \alpha x, \quad w = W_1(x,0,t), \quad N(x,0,t) = 0, \quad T(x,0,t) = T_w, \quad C(x,0,t) = C_w, \quad \text{at } z=0 \\ u(x,\infty,t) = 0, \quad N(x,\infty,t) = 0, \quad T(x,\infty,t) = T_\infty, \quad C(x,\infty,t) = C_\infty \quad \text{at } z \rightarrow \infty \end{aligned} \right\} \quad (6)$$

As a result, the no slip condition, the boundary condition  $N = 0$  at  $z = 0$  in equation (6) depicts a scenario of concentrated particle flows whereby there is no rotation of the micro-elements near the plate. The flow is along the z-axis and the inclined plate is perpendicular to the y-axis. Further,  $u$  and  $w$  represents the velocity components along the x-axis and the z-axis respectively. The mass transfer at the surface is taken as

$W_1 = -\sqrt{\frac{\nu \alpha}{2}} W_0$  while  $W_1 < 0$  denotes suction and  $W_1 > 0$  denotes injection.

### 1.3 NON-DIMENSIONALISATION

Making the values dimensionless using the following substitution:

$$\left. \begin{aligned} u^* = \frac{u}{U_0}, \quad w^* = \frac{w}{W_0}, \quad x^* = \frac{U_0}{\nu} x, \quad w^* = \frac{U_0}{\nu} w, \quad t^* = \frac{U_0^2}{\nu} t, \\ N^* = \frac{\nu}{U_0^2} N, \quad j^* = \frac{U_0^2}{\nu^2} j, \quad \theta = \frac{(T - T_\infty)}{(T_s - T_\infty)}, \quad \phi = \frac{(C - C_\infty)}{(C_s - C_\infty)} \end{aligned} \right\} \quad (7)$$

Introducing the following non-dimensional quantities which are of engineering interest;

Prandtl Number,  $Pr = \frac{\nu}{k/\rho C_p} = \frac{\nu \rho C_p}{k}$ , Grashof

Number,  $Gr = \frac{\nu g^* \beta (T_s - T_\infty)}{U_0^3}$ , Modified Grashof

Number,  $Gc = \frac{g^* \beta c \nu (C_s - C_\infty)}{U_0^3}$ ,

$\lambda = \frac{\gamma}{\rho \nu j}$ ,  $\Delta = \frac{k}{\rho \nu} = \frac{k}{\mu}$  Dimensionless material

parameters

Non-dimensionalizing equations (2)-(5) we obtain;

$$\frac{\partial u}{\partial x} + \frac{\partial w}{\partial z} = 0 \quad (8)$$

$$\begin{aligned} \frac{\partial u}{\partial t} + u \frac{\partial u}{\partial x} + w \frac{\partial u}{\partial z} = (1 + \Delta) \frac{\partial^2 u}{\partial z^2} + Gr \theta \cos \varphi + Gc \phi \cos \varphi \\ + \Delta \frac{\partial N}{\partial z} - \left( M \sin^2 \psi + \frac{1}{K} \right) u \end{aligned} \quad (9)$$

$$\frac{\partial N}{\partial t} + u \frac{\partial N}{\partial x} + w \frac{\partial N}{\partial z} = \lambda \frac{\partial^2 N}{\partial z^2} - \frac{\Delta}{j} \left\{ 2N + \frac{\partial u}{\partial z} \right\} \quad (10)$$

$$\frac{\partial \theta}{\partial t} + u \frac{\partial \theta}{\partial x} + w \frac{\partial \theta}{\partial z} = \frac{1}{Pr} \frac{\partial^2 \theta}{\partial z^2} + Ec \left( \frac{\partial u}{\partial z} \right)^2 + Du \frac{\partial^2 \phi}{\partial z^2} \quad (11)$$

$$\frac{\partial \phi}{\partial t} + u \frac{\partial \phi}{\partial x} + w \frac{\partial \phi}{\partial z} = \frac{1}{Sc} \frac{\partial^2 \phi}{\partial z^2} + Sr \frac{\partial^2 \theta}{\partial z^2} \quad (12)$$

The boundary conditions are transformed as;

$$\left. \begin{aligned} u(x,0,t) = 0, \quad N(x,0,t) = 0, \quad \theta(x,0,t) = 1, \quad \phi(x,0,t) = 1 \\ u(x,\infty,t) = 0, \quad N(x,\infty,t) = 0, \quad \theta(x,\infty,t) = 1, \quad \phi(x,\infty,t) = 1 \end{aligned} \right\} \quad (13)$$

## II. METHODOLOGY

The equations that govern the flow in porous media past a vertical semi-infinite inclined plate with heat and mass transfer in the presence of variable inclined magnetic field are coupled and highly non-linear. They are represented by equations (13), (14), (15), (16) and (17).

In this case we consider the problem of mathematical modelling of MHD unsteady heat and mass transfer of a micropolar fluid past a vertical semi-infinite porous inclined plate and magnetic field with Soret and Dufour effects. The problem is governed by a system of partial differential equations that takes the form;

$$\frac{\partial u}{\partial x} + \frac{\partial w}{\partial z} = 0 \quad (19)$$

$$\begin{aligned} \frac{\partial u}{\partial t} + u \frac{\partial u}{\partial x} + w \frac{\partial u}{\partial z} = (1 + \Delta) \frac{\partial^2 u}{\partial z^2} + Gr \theta \cos \varphi + Gc \phi \cos \varphi \\ + \Delta \frac{\partial N}{\partial z} - \left( M \sin^2 \psi + \frac{1}{K} \right) u \end{aligned} \quad (20)$$

$$\frac{\partial N}{\partial t} + u \frac{\partial N}{\partial x} + w \frac{\partial N}{\partial z} = \lambda \frac{\partial^2 N}{\partial z^2} - \frac{\Delta}{j} \left\{ 2N + \frac{\partial u}{\partial z} \right\} \quad (21)$$

$$\frac{\partial \theta}{\partial t} + u \frac{\partial \theta}{\partial x} + w \frac{\partial \theta}{\partial z} = \frac{1}{Pr} \frac{\partial^2 \theta}{\partial z^2} + Ec \left( \frac{\partial u}{\partial z} \right)^2 + Du \frac{\partial^2 \phi}{\partial z^2} \quad (22)$$

$$\frac{\partial \phi}{\partial t} + u \frac{\partial \phi}{\partial x} + w \frac{\partial \phi}{\partial z} = \frac{1}{Sc} \frac{\partial^2 \phi}{\partial z^2} + Sr \frac{\partial^2 \theta}{\partial z^2} \quad (23)$$

Eqs.20-23 are solved subject to boundary conditions

$$\left. \begin{aligned} u(x,0,t) = 0, N(x,0,t) = 0, \theta(x,0,t) = 1, \phi(x,0,t) = 1 \\ u(x,\infty,t) = 0, N(x,\infty,t) = 0, \theta(x,\infty,t) = 1, \phi(x,\infty,t) = 1 \end{aligned} \right\} \quad (24)$$

and the initial conditions

$$u(x,y,0) = 0, N(x,y,0) = 0, \theta(x,y,0) = 0, \phi(x,y,0) = 0 \quad (25)$$

Application of the Trivariate spectral collocation method results into the following numerical scheme;

$$\left( M \sin^2 \psi + \frac{1}{K} \right) \prod_k^j \left[ (1 + \Delta) \bar{D}_{j,q}^2 - w \bar{D}_{j,q} \right] \prod_k^q \sum_{r=0}^{N_x} \bar{D}_{k,r} \prod_r^q = R_1 \quad (26)$$

$$\left[ -u_{s+1} D + \frac{2\Delta}{j} I \right] N_k^j + \sum_{q=0}^{N_z} \left[ \lambda \bar{D}_{j,q}^2 - w \bar{D}_{j,q} \right] N_k^q - \sum_{r=0}^{N_x} \sum_{q=0}^{N_z} \bar{D}_{k,r} N_r^q = R_2 \quad (27)$$

$$\left[ -u_{s+1} D \right] \Theta_k^j + \sum_{q=0}^{N_z} \left[ \frac{1}{Pr} \bar{D}_{j,q}^2 - w \bar{D}_{j,q} \right] \Theta_k^q - \sum_{r=0}^{N_x} \sum_{q=0}^{N_z} \bar{D}_{k,r} \Theta_r^q = R_3 \quad (28)$$

$$\left[ -u_{s+1} D \right] \Phi_k^j + \sum_{q=0}^{N_z} \left[ \frac{1}{Sc} \bar{D}_{j,q}^2 + S \bar{D}_{j,q} \right] \Phi_k^q - \sum_{r=0}^{N_x} \sum_{q=0}^{N_z} \bar{D}_{k,r} \Phi_r^q = R_4 \quad (29)$$

where I is an identity matrix of size  $(N_x + 1) \times (N_x + 1)$ . The right-hand side of equations Eqs. (26)-(29) is defined as

$$\left. \begin{aligned} R_1 = -u_s \frac{\partial u_s}{\partial x} - Gr \cos \phi \theta_s - Gc \cos \phi \phi_s - \Delta \frac{\partial N_s}{\partial z}, R_2 = -\frac{\Delta}{j} \frac{\partial u_{s+1}}{\partial z} \\ R_3 = -Ec \left( \frac{\partial u_{s+1}}{\partial z} \right)^2 - Du \frac{\partial^2 \phi_s}{\partial z^2}, R_4 = -Sr \frac{\partial^2 \theta_{s+1}}{\partial z^2} \end{aligned} \right\} \quad (30)$$

The numerical scheme Eqs. (26)-(29) is solved subject to the boundary conditions

$$\left. \begin{aligned} u_{s+1}(x, zN_z, t) = 0, N_{s+1}(x, zN_z, t) = 0, \theta_{s+1}(x, zN_z, t) = 1, \phi_{s+1}(x, zN_z, t) = 1 \\ u_{s+1}(x, z_0, t) = 0, N_{s+1}(x, z_0, t) = 0, \theta_{s+1}(x, z_0, t) = 1, \phi_{s+1}(x, z_0, t) = 1 \end{aligned} \right\} \quad (31)$$

to yield the approximate numerical solution.

### 2.1 PARAMETER CONSIDERATION

The various parameters that have been varied include the Schmidt number  $Sc$ , Soret number  $Sr$ , Magnetic field  $M$ , Material parameter  $K$ , Micropolar parameter  $\Delta$ , Grashof number  $Gr$ , Modified Grashof number  $Gm$ , time  $t$ , Dufour number  $Du$ , Suction parameter  $S$ , Nusselt number  $Nu$ , Eckert number  $Ec$ , Prandtl number  $Pr$ , and Injection parameter  $w_0$ . These parameters are input into a MATLAB computer program where each parameter is varied at a time.

### 2.2 NUSSLT NUMBER, SHERWOOD NUMBER AND LOCAL SKIN-FRICTION COEFFICIENT

The quantities of main engineering interest in the problem at hand are the Nusselt number, the Sherwood number, and the shearing stress on the plate. The Nusselt number and the Sherwood number physically indicate the rate of heat transfer and the rate of mass transfer respectively. The equation defining the wall shear stress is

$$\tau_w = (\mu + k) \left( \frac{\partial u}{\partial z} \right)_{z=0} + kN(z)_{z=0} \quad (32)$$

Thus, Skin Friction Coefficient,  $C_f$ , is computed as

$$\begin{aligned} C_f &= \frac{2\tau}{\rho U_0^2} = \frac{2(\mu + k)}{\rho U_0^2} \left( \frac{\partial u}{\partial z} \right)_{z=0} = \frac{2}{U_0^2} [v + \Delta v] \left( \frac{\partial u}{\partial z} \right)_{z=0} \\ &= \frac{2}{U_0^2} [1 + \Delta] v \left( \frac{\partial u}{\partial z} \right)_{z=0} \end{aligned} \quad (33)$$

The above relation shows that the skin friction coefficient  $C_f$  is proportional to

$$\frac{1}{U_0^2} [1 + \Delta] v \left( \frac{\partial u}{\partial z} \right)_{z=0} \quad (34)$$

The Heat flux at the surface is calculated as

$$q_w = -\kappa \left( \frac{\partial T}{\partial z} \right)_{z=0} \quad (35)$$

The rate of heat transfer in terms of the Nusselt number at the plate is given by

$$Nu_x = \frac{-\kappa \left( \frac{\partial T}{\partial z} \right)_{z=0} \left( \frac{x}{\kappa} \right)}{(T_w - T_\infty) \left( \frac{x}{\kappa} \right)} = \frac{q_w}{(T_w - T_\infty) \left( \frac{x}{\kappa} \right)} \quad (36)$$

The mass flux is defined as follows

$$m_w = -D_M \left( \frac{\partial C}{\partial z} \right)_{z=0} \quad (37)$$

The rate of mass transfer in terms of the dimensionless Sherwood number is defined as follows

$$Sh_x = \frac{-x D_M \left( \frac{\partial C}{\partial z} \right)_{z=0}}{D_M (C_w - C_\infty)} = \frac{x m_w}{D_M (T_w - T_\infty)} \quad (38)$$

In the present study, the following default parametric

values are adopted:  $M = 0.5$ ,  $\psi = \frac{\pi}{2}$ ,  $\phi = \frac{\pi}{6}$ ,

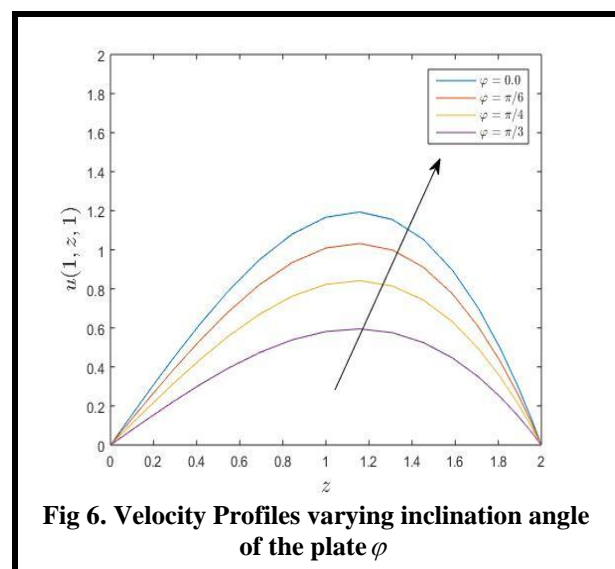
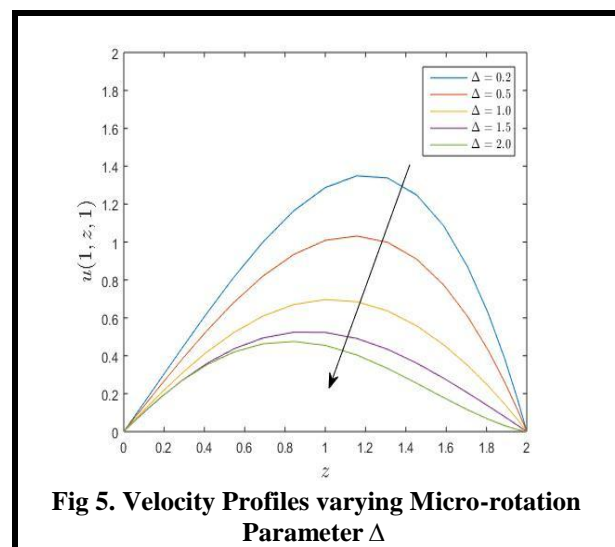
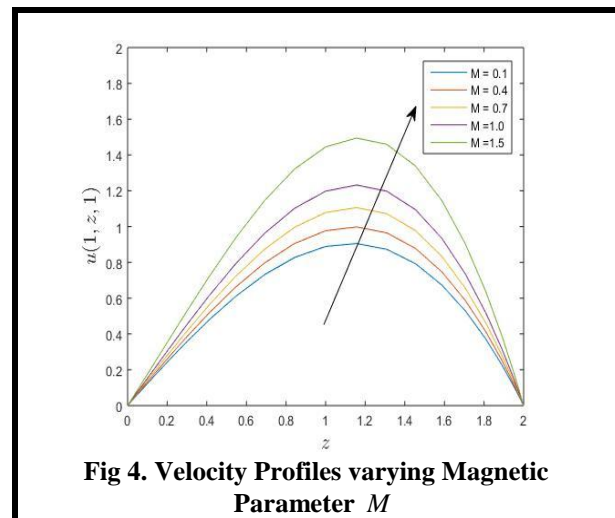
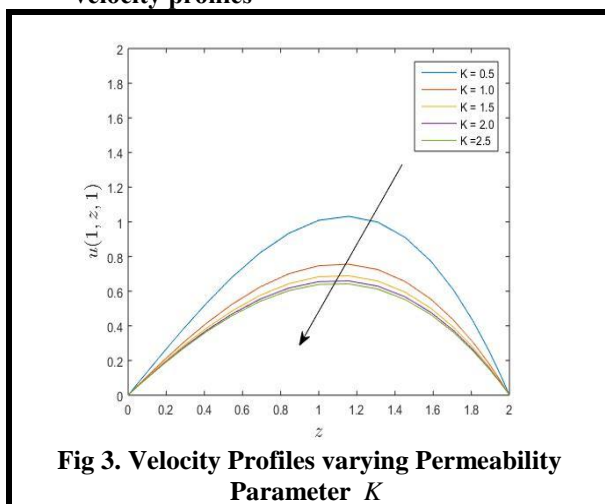
$S = 1.0$ ,  $Ec = 0.01$ ,  $Gc = 2$ ,  $Sr = 1.0$ ,  $Du = 0.1$ ,  $B = 0.5$ ,  $\lambda = 0.2$ ,  $\Delta = 0.5$ ,  $Gr = 1.00$ ,  $Pr = 0.71$ ,  $J = 1.00$ ,  $Sc = 0.22$ ,  $\alpha = 0.5$  in all graphs. The values of Dufour number and Soret number are chosen in such a way that their product is constant provided that the mean temperature  $T_m$  is constant as well.

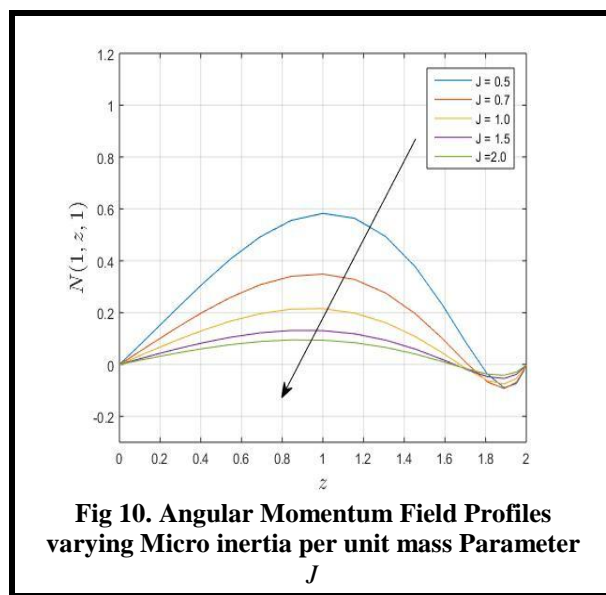
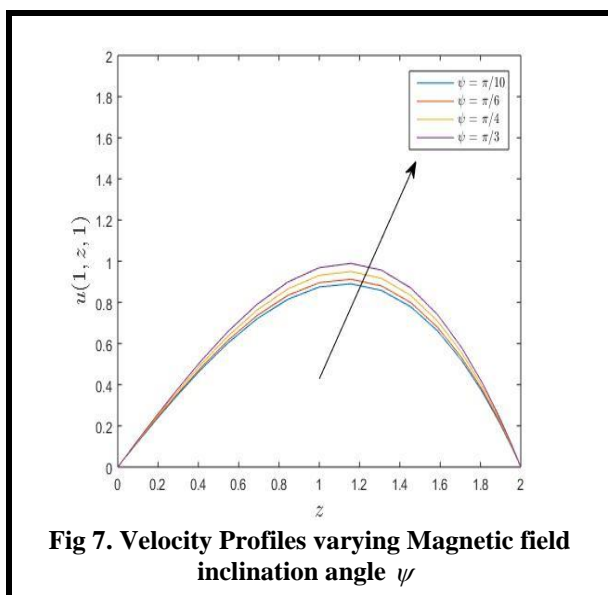
## III. RESULTS AND DISCUSSION

The effects of Soret and Dufour on unsteady MHD heat and mass transfer of a Micropolar fluid past a vertical semi-infinite porous inclined plate in presence of an inclined Magnetic field is also investigated. Using the aforementioned numerical procedure, the numerical results obtained using the governing equations (38) -(41) subject to the boundary conditions (42) and (26) -(29) together with the boundary equations are displayed through graphs and tables below. To study the physical situation of these problems, we have computed the numerical values of the velocities, angular momentum, temperature, concentration, within the boundary layer and also found the skin friction coefficients, Nusselt and Sherwood number at the plate. It can be seen that the solutions are affected by the non-dimensional parameters and numbers, namely suction parameter  $S$ , local Grashof number  $Gr$ , local modified Grashof number  $Gc$ , permeability parameter  $K$ , Magnetic parameter  $M$ , Prandtl number  $Pr$ , Eckert number  $Ec$ , Dufour number  $Du$ , Schmidt number  $Sc$ , Soret number  $Sr$ , heat source parameter  $\alpha$ , Micro inertia per unit mass  $J$ , Material parameter  $\kappa$ , Nusselt number  $Nu$ , Sherwood number  $Sh_x$  and dimensionless material (Micropolar) parameter  $\Delta$ . The numerical solutions regarding the velocity, angular momentum, temperature and concentration distributions are presented for different selected values of the established dimensionless parameters. The influences of these various parameters on the velocity angular momentum, temperature and concentration fields are presented in Figure1 through Figure 20 and some of the numerical results regarding coefficients skin friction and heat transfer are given in tabular form in Table 1 and Table 2. The results are discussed in section 3.3, 3.4 and 3.5.

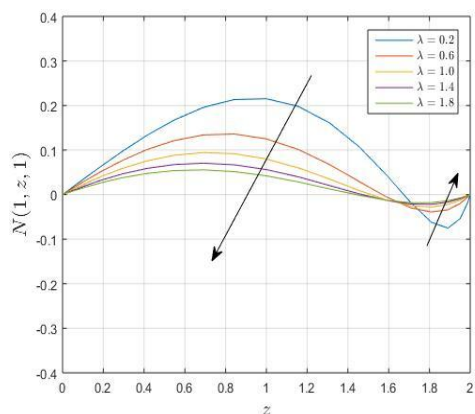
### 3.1 Results

#### 3.1.1 Effect of various parameters on the velocity profiles





3.1.2 Angular Momentum Field Profiles



3.1.3 Temperature Field Profiles

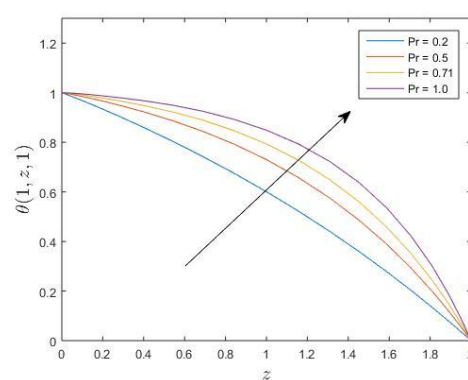


**Fig 8. Angular Momentum Field Profiles varying Dimensionless Material Parameter  $\lambda$**

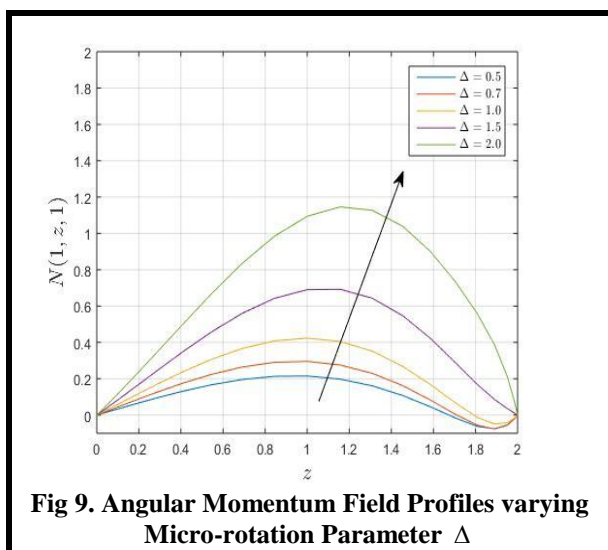


**Fig 11. Temperature Profiles varying Prandtl Number  $Pr$**

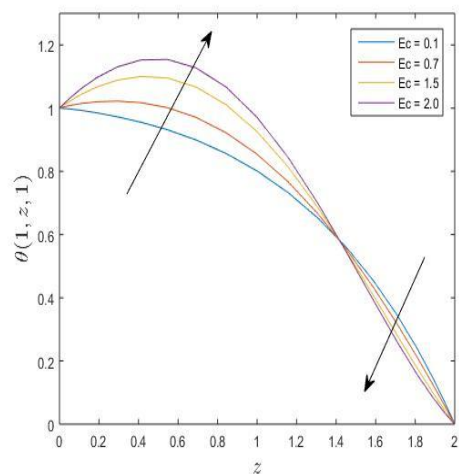


**Fig 12. Temperature Profiles varying Eckert Number  $Ec$**

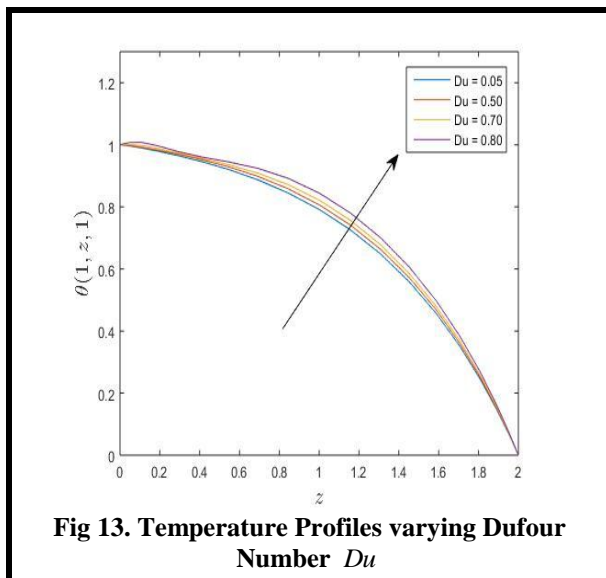


Fig 13. Temperature Profiles varying Dufour Number  $Du$

5.1.4 Concentration Field Profiles

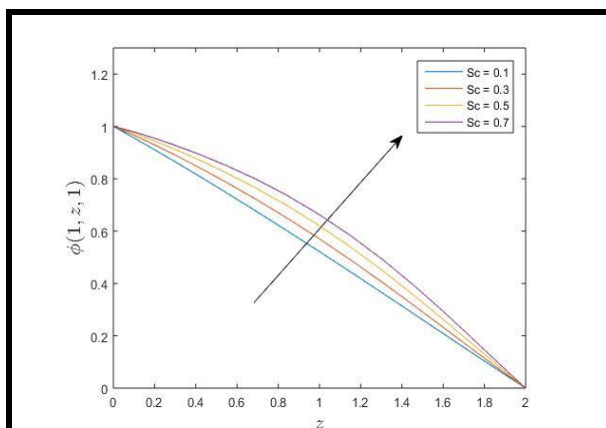


Fig 14. Concentration Profiles varying Schmidt Number  $Sc$

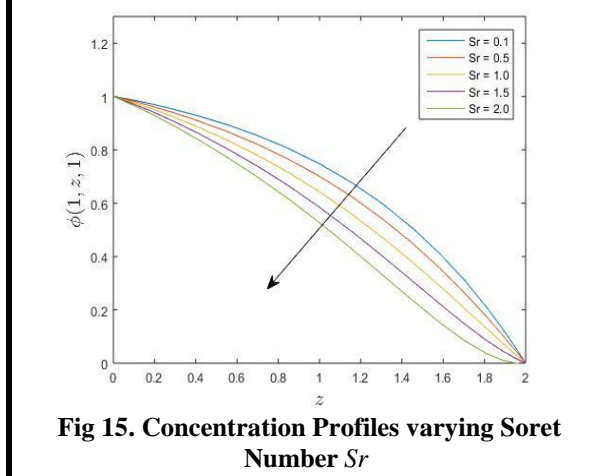


Fig 15. Concentration Profiles varying Soret Number  $Sr$

3.1.4 Computed values of skin friction, the local Nusselt number and Sherwood number

In the following the effect of different parameters on the coefficient of skin friction Nusselt number and Sherwood Number are tabulated in table (1) - (6). The values shown there are proportional to the coefficient of skin friction, Nusselt number and Sherwood number.

TABLE 1

Values of  $Cf_x, Nu_x, Sh_x$  for different values of  $Du$

$Du$	Present study			Lakshmi, K.B (2018)		
	$Cf_x$	$Nu_x$	$Sh_x$	$Cf_x$	$Nu_x$	$Sh_x$
0.1	4.05345	-	-	1.01336	-	-
		0.06079	0.21432		0.43128	0.30571
0.3	4.05184	-	-	1.01296	-	-
		0.05220	0.21735		1.29384	0.32424
0.5	4.04770	-	-	1.01193	-	-
		0.03585	0.22665		2.15640	0.37070
0.7	4.03827	-	-	1.00956	-	-
		0.06500	0.29713		2.87512	0.37486
1.0	4.00098	-	-	1.00025	-	-
		2.62496	2.21935		3.14580	0.37510

TABLE 2

Values of  $Cf_x, Nu_x, Sh_x$  for different values of  $Sr$

$Sr$	Present study			Lakshmi, K.B (2018)		
	$Cf_x$	$Nu_x$	$Sh_x$	$Cf_x$	$Nu_x$	$Sh_x$
0.1	4.12876	-	-	1.03219	-2.0860	-
		0.05844	0.10934			0.70220
0.5	4.09385	-	-	1.02346	-	-
		0.05966	0.15606		2.11950	0.71770
1.0	4.05345	-	-	1.01336	-	-
		0.06079	0.21432		2.23492	0.78552
1.5	4.01495	-	-	1.00374	-	-
		0.06133	0.27246		2.23552	0.82726
2.0	3.97630	-	-	0.99408	-	-
		0.06119	0.33039		2.23671	0.84238

TABLE 3

Values of  $Cf_x, Nu_x, Sh_x$  for different values of  $\phi$

$\phi$	Present study			Wahiduzzaman, M. et al. (2015)		
	$Cf_x$	$Nu_x$	$Sh_x$	$Cf_x$	$Nu_x$	$Sh_x$
0	4.43	-	-	3.282	-0.96	-
.	904	0.060	0.21	5601	86241	0.6969
0		52	446			894
$\frac{\pi}{6}$	3.84	-	-	2.977	-0.99	-
	299	0.061	0.21	8622	41611	0.6795
		02	424			973
$\frac{\pi}{4}$	3.13	-	-	2.583	-1.03	-
	678	0.061	0.21	5102	28613	0.6551
		62	398			832
$\frac{\pi}{6}$	2.21	-	-	2.020	-1.10	-
	749	0.062	0.21	6484	38032	0.6158
		41	364			846

**TABLE 4**

Values of  $Cf_x$ ,  $Nu_x$ ,  $Sh_x$  for different values of  $\psi$

$\psi$	Present study			Hayat et al. (2015)		
	$Cf_x$	$Nu_x$	$Sh_x$	$Cf_x$	$Nu_x$	$Sh_x$
$\frac{\pi}{10}$	3.72452	-0.06115	0.21419	3.13268	-0.64028	-0.42838
$\frac{\pi}{6}$	3.76268	-0.06111	0.21421	3.1465	-0.64016	-0.42842
$\frac{\pi}{4}$	3.84299	-0.06102	0.21424	3.16996	-0.63998	-0.42848
$\frac{\pi}{3}$	4.05345	-0.06079	0.21432	3.19197	-0.63376	-0.42864

### 3.2 Discussion

#### 3.2.1 Velocity Profiles

From Figure 1, Velocity  $u$  decreases significantly on increasing Permeability Parameter  $K$ . Thus, increasing values of  $K$  respond to the large opening of the porous space, which reduces retardation of the flow thereby reducing the velocity. We observe that the magnitude of the stream wise velocity decreases and the inflection point for the velocity distribution moves further away from the surface.

Form Figure 2, Velocity  $u$  increases significantly on increasing the Magnetic parameter  $M$ . The effect of growing magnetic parameter is to retard the main velocity of the flow field due to the magnetic pull of the Lorentz force acting on the flow field. The higher value of  $M$ , the more prominent is the enhancement in velocity. From Figure 3, Velocity  $u$  decreases significantly on increasing micro-rotation parameter  $\Delta$ . This is because the micro-rotation increases very rapidly with the increase of the vortex viscosity parameter  $\Delta$ . It is also understood that as the vortex viscosity increases the rotation of the micropolar constituents gets induced in most part of the boundary layer except very close to the wall where kinematic viscosity dominates the flow.

Form Figure 4, Velocity  $u$  increases significantly on increasing the inclination angle of the plate  $\phi$ . When  $\phi$  increases, the normal component of the buoyancy force decreases near the leading edge, which causes an impulsive driving force to fluid motion along the plate. That is, the impulsive force along the plate decreases with increasing  $\phi$ .

Form Figure 5, Velocity  $u$  increases significantly on increasing the inclination angle of the Magnetic field  $\psi$ . It is due to the fact that with an increase in angle of inclination, the effect of magnetic field on fluid particles increases which enhances the Lorentz force. Consequently, the velocity profile decreases. Furthermore, the angle of inclination tends to increase mass flow rate in fluid

flow direction. In fact higher values of angle  $\psi$  corresponds to larger magnetic field which opposes the fluid motion.

#### 3.2.2 Angular Momentum Field Profiles

From Figure 6, angular momentum  $N$  decreases significantly on increasing dimensionless material parameter  $\lambda$ . It is noted that initially the micro-rotation/angular velocity  $N$  decreases but after  $\eta = -0.5$ , it goes to increase for large values of  $\lambda$ . The boundary layer thickness is decreased as the vortex viscosity  $\lambda$  increases. Meanwhile, the angular velocity in Figure 6 decreases with the increment of  $\lambda$  for the first solution even though there is an increase in the gyration on the surface initially. In other words, the fluid moves rapidly on the surface in a whirling motion. Moreover, there is a point where the angular velocity profiles intersect near the surface (approximately  $\eta = -0.5$ ) for the first solution. This indicates that this layer presents a transition state after which the opposite effect, i.e.  $|h(\eta)|$  increases with an increasing  $\lambda$  till the free stream state is attained. It shows that near the solid surface, the effect of micro-rotation is more pronounced for the first solution compared to that of the second solution.

From Figure 7, angular momentum  $N$  increases significantly in the negative values on increasing Micropolar parameter  $\Delta$ . It is also understood that as the vortex viscosity increases the rotation of the micropolar constituents gets induced in most part of the boundary layer except very close to the wall where kinematic viscosity dominates the flow.

From Figure 8, angular momentum  $N$  decreases significantly on increasing the Micro inertia per unit mass Parameter  $J$ . The reason is because the viscous friction within the fluid tends to organize the flow into a collection of irrotational vortices and a moving vortex carries with it some angular and linear momentum and energy.

#### 3.2.3 Temperature Field Profiles

From Figure 9, Temperature  $\theta$  monotonically increases on increasing Prandtl number  $Pr$ .  $Pr$  is the ratio of momentum to thermal diffusivities. Thus, increasing  $Pr$  implies that momentum and viscous diffusion dominates the flow rather than thermal diffusion. This is as expected because the increasing of Prandtl number will affect the kinematic viscosity and thermal diffusivity of the fluid.

From Figure 10, Temperature  $\theta$  monotonically increases on

increasing Eckert number  $Ec$  and crosses over the profiles since internal energy is increased due to kinetic energy dissipation.  $Ec$  expresses the relationship between the kinetic energy in the flow and the boundary layer enthalpy difference. It embodies the conversion of kinetic energy into internal energy by work done against the viscous fluid stresses. It is an important parameter for describing real working fluids in MHD energy generators and materials processing where dissipation effects are not trivial. Positive Eckert number corresponds to cooling of the wall (plate) and therefore a transfer of heat from the plate to the micropolar fluid. Convection is enhanced and we observe in consistency with that the fluid is accelerated i.e. linear (translational) velocity is increased in the micropolar fluid.

From Figure 11, Temperature  $\theta$  monotonically increases on increasing Dufour number  $Du$ . This is because the  $Du$  effects reduce the growth of the momentum boundary layer and increases the growth of thermal boundary layer.

### 3.2.4 Concentration Field Profiles

From Figure 12, Concentration  $\phi$  monotonically decreases on increasing Schmidt parameter  $Sc$ .  $Sc$  represents the ratio between the momentum diffusivity (linked to  $\nu$ ) and the mass diffusivity (linked to  $D_B$ ). It physically relates the relative thickness of the hydrodynamic layer and mass-transfer boundary layer. Thus, a lower value of Schmidt number indicates a thicker boundary layer. At high  $Sc$ , particles are giant, with small diffusivity, and this kind of deposition becomes less and less relevant, thus decreasing the concentration profiles. Concentration boundary layer thickness is therefore significantly reduced with greater Schmidt number. Smaller values of  $Sc$  are equivalent to increasing the chemical molecular diffusivity and vice versa for larger values of  $Sc$ .

From Figure 13, Concentration  $\phi$  monotonically decreases on increasing Soret number  $Sr$ . Increasing the Soret number ( $Sr$ ) increases the boundary layer thickness for the concentration that consequently decreases the concentration boundary layer thus reducing the concentration distribution.

### 3.2.5 Skin friction $Cf_x$ , the local Nusselt number $Nu_x$ and Sherwood number $Sh_x$

From tables 1, 2, 3 and 4, an increase in the parameters  $Du$ ,  $Sr$ ,  $\phi$  and  $\psi$  results in decrease in  $Cf_x$ .

In table 1 and 4, increase in  $Du$  and  $\psi$  results to a decrease in  $Nu_x$ . Heat transfer rates

decrease with increase in  $Du$  because the heat generation mechanism increases the temperature of the fluid near the surface of the sheet.

In tables 1, 2 and 4, increase in  $Du$ ,  $Sr$  and  $\psi$  increases  $Sh_x$  while an increase in  $\phi$  decreases  $Sh_x$  (table 3).

## IV. CONCLUSION

A conclusion section must be included and should indicate clearly the advantages, limitations, and possible applications of the paper. Although a conclusion may review the main points of the paper, do not replicate the abstract as the conclusion. A conclusion might elaborate on the importance of the work or suggest applications and extensions.

Mathematical Modelling of MHD Unsteady heat and mass transfer of a Micropolar fluid past a vertical semi-infinite porous inclined plate and magnetic field with Soret and Dufour effects has been investigated. It is concluded that;

- i. Velocity distributions increases on increasing  $M$ ,  $\phi$ ,  $\psi$  but decreases on increasing  $K$ ,  $\Delta$ .
- ii. The angular momentum profiles rises after crossing over negative values on increasing  $\lambda$ ,  $\Delta$  but falls after crossing the positive values on increasing  $\lambda$  and  $J$ .
- iii. Temperature profiles rises on enhancing  $Pr$ ,  $Ec$ ,  $Du$  but decreases slightly towards  $\theta = 0$  on increasing  $Du$ .
- iv. Concentration profiles increases on increasing  $Sc$  but decreases on increasing  $Sr$
- v. Skin friction  $Cf_x$  increases with increasing  $\psi$  but falls on enhancing  $Du$ ,  $Sr$  and  $\phi$
- vi. Nusselt number  $Nu_x$  increases on enhancing  $Du$ ,  $Sr$ ,  $\phi$  but  $Nu_x$  falls with increasing  $\psi$ .
- vii. Sherwood number  $Sh_x$  rises on increasing  $Du$ ,  $Sr$ ,  $\psi$  but falls on increasing  $\phi$

From the results reported in the present research, it is evident that the results are in good agreement with general published trends. This follows the physical expectation of the effect of various parameters. As elucidated in section three physical trends were eminent in the results.

## ACKNOWLEDGEMENTS

The authors wish to thank National Commission for Science, Technology and Innovation. This work was supported in part by a grant from National Commission for Science, Technology and Innovation.

## REFERENCES

- [1]. Borgohain, B. (2015). Micropolar fluid over a stretching surface in a non-Darcian porous medium when viscosity and thermal conductivity vary with temperature in presence of magnetic field, *International Research Journal of Mathematics, Engineering and IT*, 2(10), ISSN: (2349-0322)
- [2]. Eringen, A. C. (1972). Theory of thermomicrofluids. *Journal of Mathematical Analysis and Applications*, 38(2), 480-496.
- [3]. Lukaszewicz, G. (1999). *Micropolar fluids: theory and applications*. Springer Science & Business Media.
- [4]. Koriko, O. K., Omowaye, A. J., Animasaun, I. L., & Bamsaye, M. E. (2017). Melting heat transfer and induced-magnetic field effects on the micropolar fluid flow towards stagnation point: Boundary layer analysis. In *International Journal of Engineering Research in Africa*, 29, 10-20. Trans Tech Publications.
- [5]. Maraka, W. M., Ngugi, K. M., & Roy, K. P. (2018). Similarity Solution of Unsteady Boundary Layer Flow of Nanofluids past a Vertical Plate with Convective Heating. *Global Journal of Pure and Applied Mathematics*, 14(4), 517-534.
- [6]. Baruah, I., & Hazarika, G. C. (2017). Effects of Variable Viscosity and Thermal Conductivity of Unsteady Micropolar Fluid under Mixed Convection in Presence of Uniform Magnetic Field on Stretching Surface. *International Journal of Computer Applications*, 166(3).
- [7]. Govardhan, K., Nagaraju, G., Kaladhar, K., & Balasiddulu, M. (2015). MHD and radiation effects on mixed convection unsteady flow of micropolar fluid over a stretching sheet. *Procedia Computer Science*, 57, 65-76.
- [8]. Atif, S. M., Hussain, S., & Sagheer, M. (2018). Numerical study of MHD micropolar carreau nanofluid in the presence of induced magnetic field. *AIP Advances*, 8(3), 035219.
- [9]. Mohammad, A., & Mohammad, S. A. (2013). Soret and Dufour Effects on Steady Free Convective in MHD Micropolar Fluid Flow, Mass and Heat Transfer with Hall Current. *International Journal of Advancements in Research and Technology*, 2, 130-138.
- [10]. Rashid, G. M. (2012). *Transient Free Convection in Micropolar Fluid with Heat Generation and Constant Heat Flux* (Doctoral dissertation, Khulna University of Engineering & Technology (KUET), Khulna, Bangladesh.).
- [11]. Haque, M. Z., Alam, M. M., Ferdows, M., & Postelnicu, A. (2012). Micropolar fluid behaviours on steady MHD free convection and mass transfer flow with constant heat and mass fluxes, joule heating and viscous dissipation. *Journal of King Saud University-Engineering Sciences*, 24(2), 71-84.
- [12]. Uwanta, I. J., & Usman, H. (2014). On the Influence of Soret and Dufour Effects on MHD Free Convective Heat and Mass Transfer Flow over a Vertical Channel with Constant Suction and Viscous Dissipation. *International scholarly research notices*.
- [13]. Reddy, L. R., Raju, M. C., Raju, G. S. S., & Ibrahim, S. M. (2017). Chemical reaction and thermal radiation effects on MHD micropolar fluid past a stretching sheet embedded in a non-Darcian porous medium. *Journal of Computational and Applied Research in Mechanical Engineering*, 6(2), 27-46.
- [14]. Lakshmi, K. B., Sugunmama, V., Reddy, J. R., (2018). Effect of Soret and Dufour Numbers on Chemically Reacting Powell-Eyring Fluid Flow over an Exponentially Stretching Sheet. *Int. Journal of Engineering Research and Application*, 8(4), 61-72
- [15]. Wahiduzzaman, M., Biswas, R., Ali, M. E., Khan, M. S., & Karim, I. (2015). Numerical Solution of MHD Convection and Mass Transfer Flow of Viscous Incompressible Fluid about an Inclined Plate with Hall Current and Constant Heat Flux. *Journal of Applied Mathematics and Physics*, 3(12), 1688.
- [16]. Hayat, Anum Shafiq, A. Alsaedi, and S. Asghar, (2015). Effect of inclined magnetic field in flow of third grade fluid with variable thermal conductivity, *AIP Advances*, 5(8), 087108 1-15

Mutua Nicholas Muthama" Mathematical Modelling of MHD Unsteady heat and mass transfer of a Micropolar fluid past a vertical semi-infinite porous inclined plate and magnetic field with Soret and Dufour effects" *International Journal of Engineering Research and Applications (IJERA)*, Vol. 09, No.03, 2019, pp. 47-56